

# Exosomal miR-211 derived from cancer stem cells promotes cancer progression by activating autophagy in NSCLC

Xiaoxue Zhang<sup>1</sup>, Yan Chen<sup>2</sup>, Yongchao Yu<sup>3</sup>, Shu Zhu<sup>1</sup>, Jing Zhang<sup>1</sup>, Yan Wang<sup>1</sup>, Xiangyun Zhang<sup>1</sup>

<sup>1</sup>Department of Oncology, Hiser Medical Center of Qingdao, Qingdao 266001, Shandong Province, China

<sup>2</sup>Department of Urologic Surgery, Hiser Medical Center of Qingdao, Qingdao 266001, Shandong Province, China

<sup>3</sup>Department of Intervention, Hiser Medical Center of Qingdao, Qingdao 266001, Shandong Province, China

**Correspondence to:** Xiangyun Zhang; email: [xiaoshui0816@163.com](mailto:xiaoshui0816@163.com)

**Keywords:** NSCLC, exosome, CSC, miR-211, autophagy

**Received:** March 28, 2020

**Accepted:** June 29, 2020

**Published:**

**Copyright:** © 2020 Zhang et al. This is an open access article distributed under the terms of the [Creative Commons Attribution License](https://creativecommons.org/licenses/by/3.0/) (CC BY 3.0), which permits unrestricted use, distribution, and reproduction in any medium, provided the original author and source are credited.

## ABSTRACT

**Background:** Non-small cell lung cancer (NSCLC) has the highest clinical incidence in all of types lung cancer, which seriously affects people's lives and increases the financial burden of medical care. Therefore, it is crucial to identify the molecular mechanisms and pathways of lung cancer occurrence and development, and find more effective treatment methods and targeted drugs.

**Results:** MiR-211 was highly expressed in CSC exosomes, and exosomal miR-211 mainly derived from CSCs in NSCLC. CSCs exosomes co-cultured with NSCLC cells promoted the viability, migration and invasion of NSCLC cells. Furthermore, exo-miR-211 promoted NSCLC cells autophagy, and inhibition of autophagy with autophagy inhibitor 3-MA reversed CSC-derived exo-miR211 promoting effects on NSCLC progression. Further analysis showed BCL-W was a direct target of miR-211, and miR-211 facilitated cancer progression and autophagy in NSCLC cells via BCL-W inhibition. *In vivo* tumorigenesis assay showed CSC-derived exo-miR-211 enhanced NSCLC progression and promoted autophagy.

**Conclusion:** Our study suggested CSCs derived exo-miR-211 promoted NSCLC progression by activating autophagy via targeting BCL-W, which might provide a new idea for NSCLC treatment.

## INTRODUCTION

In recent years, lung cancer had a high prevalence and an increasing incidence. Its mortality rate ranks first among various malignant tumors [1]. About 1.3 million people worldwide die from lung cancer each year, and nearly one third of new lung cancer cases in China [2]. Non-small cell lung cancer (NSCLC) has the highest clinical incidence in all types lung cancer, which seriously affects people's life and increases the financial burden of medical care [3]. Therefore, it is crucial to identify the molecular mechanisms and pathways of lung cancer occurrence and development, and find more effective treatment methods and targeted drugs.

Autophagy is a lysosomal-dependent protein degradation process, which maintains the internal environment's balance and homeostasis through the degradation and

recycling of proteins and damaged organelles [4]. Autophagy is closely related to lung cancer. Studies have found that in the tumorigenic processes can lead to impaired autophagy, while impaired or inhibited autophagy can cause genomic instability, interfere with cell differentiation, affect the activation of cell aging programs, and disrupt cell metabolism [5]. In turn, impaired autophagy is a potential tumorigenic process [6, 7]. Although autophagy is often impaired in the early stages of tumorigenesis, autophagy resumes in the late stages of tumor progression, and restored autophagy enables tumor cells to cope with endogenous stress and increases the need for chemotherapy or radiotherapy resistance [8].

Living cells release different types of extracellular vesicles into the extracellular environment for intercellular communication. According to their

biological phenotypes, there are mainly three types of extracellular vesicles: microvesicles, apoptotic bodies and exosomes [9]. Microvesicles are formed by budding of the cell membrane directly outward, apoptotic bodies are formed by fragments of apoptotic cell membrane cleavage, and exosomes originally originated from the endocytosis process [10]. Interestingly, exosomes have many and complex components, and contain many biological macromolecules [11]. It was reported that miRNAs existed in exosomes regulate the expression of oncogenes or tumor suppressor genes and participate in cell differentiation, apoptosis and cell signal transduction guide [12]. At the same time, exosomes can be captured by nearby cells or secreted into the blood by paracrine flow to distant organs. The proteins and nucleic acids carried by exosomes also reach the nearby and distant cells along with the exosomes, which affects the physiological or pathological processes of the recipient cells [13]. Cancer stem cells (CSCs) are involved in tumor development. It has been reported that CSCs can re-initiate and repopulate new tumor cells to promote tumor development and recurrence, which is considered as a mechanism for the tumor metastasis [14, 15].

Studies have shown that exosomes are related to the autophagy process of malignant tumors [16]. On the one hand, exosomes can regulate autophagy. On the other hand, Atg (autophagy related gene) can regulate the release of exosomes. MiR-7-5p in exosomes was found to induce recipient cell autophagy, and exosomes-mediated autophagy was significantly attenuated by miR-7-5p inhibitors. In addition, exosomes miR-7-5p-induced autophagy is associated with epidermal growth factor receptor / PI3K / Akt / mTOR signaling pathways [17]. Further research shows that miR-7-5p can target the inhibition of NOVA2 expression, thereby inhibiting the growth of NSCLC [18]. In addition, it has been shown that miR-211 can be packaged by exosomes [19], and miR-211 played a key role in various cancer [20]. However, the role of exosomal miR-211 in NSCLC cells and the underlying mechanism remains unclear.

Present study aimed to reveal the novel role of exosomal miR-211 derived from CSCs and provide new ideas for clinical treatment of NSCLC.

## RESULTS

### Exosomal miR-211 derived from CSCs in NSCLC

Firstly, we isolated cancer stem cells (CSCs) from NSCLC cancer tissue, immunofluorescence assay was performed to identify the markers CD105 and Nestin for CSCs (Figure 1A). Then, we performed qRT-PCR analysis to determine miR-211 expression tumor cells (TCs) and CSCs. The expression of miR-211 was the

highest in CSCs (Figure 1B). Furthermore, exosomes in TCs and CSCs were isolated. TEM data showed the morphology of exosomes (Figure 1C), and exosomes markers were detected by western blot (Figure 1D). Interestingly, miR-211 was the highest in CSC exosomes compared with TC exosomes (Figure 1E). These data indicated exosomal miR-211 (exo-miR-211) mainly derived from CSCs.

### Exo-miR-211 derived from CSCs accelerated cancer progression of NSCLC cells

To evaluate the role of exo-miR-211 NSCLC development, A549 and H1299 cells were incubated with exosomes isolated from CSCs transfected miR-211 or AMO-211 or its NC. And we found that miR-211 expression was significantly upregulated upon incubation with exosomes from CSCs with miR-211 overexpression but not with CSCs with antisense morpholino oligonucleotide of miR-211 (AMO-211) in A549 and H1299 cells (Figure 2A). Functionally, we performed CCK8 assay to estimate cell viability. It showed that CSCs transfected with miR-211 increased cell viability, while knockdown of miR-211 decreased cell viability in A549 and H1299 cells (Figure 2B). Furthermore, wound healing assay suggested that CSCs transfected with miR-211 promoted cell migration in A549 and H1299 cells (Figure 2C), but CSCs transfected with AMO-211 showed an opposite effect (Figure 2D). Transwell assay showed that CSCs transfected with miR-211 induced cell invasion in A549 and H1299 cells (Figure 2E), but CSCs transfected with AMO-211 showed an opposite effect (Figure 2F). In addition, overexpression of miR-211 inhibited apoptosis of A549 and H1299 cells (Figure 2G), while silencing miR-211 accelerated apoptotic ability (Figure 2H). Together, exo-miR-211 secreted by CSCs promoted tumor progression in NSCLC cells.

### Exo-miR-211 promoted cancer progression by activating autophagy of NSCLC cells

It has been proved that autophagy promotes tumorigenesis when the tumor has been formed [21], and we examined the effect of exo-miR-211 on autophagy. A549 and H1299 cells were transfected with GFP-mRFP LC3 plasmid with miR-211 or AMO-211, and confocal microscope analysis showed miR-211 promoted autophagosomes formation, while AMO-211 inhibited autophagosomes formation (Figure 3A). In addition, we tested autophagy associated gene p62 and LC3. Western blot analysis showed CSCs transfected with miR-211 inhibited p62 expression and increased LC3-II expression, while CSCs transfected with AMO-211 showed the opposite effect in A549 and H1299 cells (Figure 3B). To clarify whether exo-miR-211

promotes NSCLC progression through activating autophagy, we used autophagy inhibitor 3-MA and autophagy inducer Rapamycin. Functional experiments showed that 3-MA removed the promoted effect of CSCs transfected with miR-211 on migration and invasion in A549 and H1299 cells (Figure 3C, 3D). On the contrary, Rapamycin recovered the inhibited effect of CSCs transfected with AMO-211 on migration and invasion in A549 and H1299 cells (Figure 3E, 3F). These data indicated that exosomal miR-211 derived from CSCs promoted NSCLC development via activating autophagy.

### BCL-W was direct target of miR-211

To further clarify the downstream of miR-211, we used Targetscan to predict targets gene. Data showed that the 3'UTR of BCL-W possessed paired bases with miR-211 (Figure 4A). What's more, miR-211 significantly inhibited BCL-W expression, while AMO-211 increased BCL-W expression in A549 and H1299 cells

(Figure 4B). As expected, CSC exosomes obviously suppressed BCL-W expression in A549 and H1299 cells (Figure 4C). To investigate whether miR-211 targeted on BCL-W, we performed dual-luciferase reporter assay in HEK293 cell line. We found that the luciferase activity of WT 3'UTR of BCL-W was significantly repressed in the miR-211 group compared with NC group, while miR-211 had no effect on the luciferase activity of mutant 3'UTR of BCL-W (Figure 4D). Similarly, AMO-211 promoted the luciferase activity of WT 3'UTR of BCL-W but not the mutant 3'UTR of BCL-W (Figure 4D). As expected, CSC exosomes also effectively downregulated the luciferase activity of WT 3'UTR of BCL-W (Figure 4E).

### Exo-miR-211 accelerated NSCLC development via BCL-W downregulation

To further elucidate the functional role of the BCL-W in miR-211 promoting NSCLC development, A549 and H1299 cells were transfected with BCL-W or

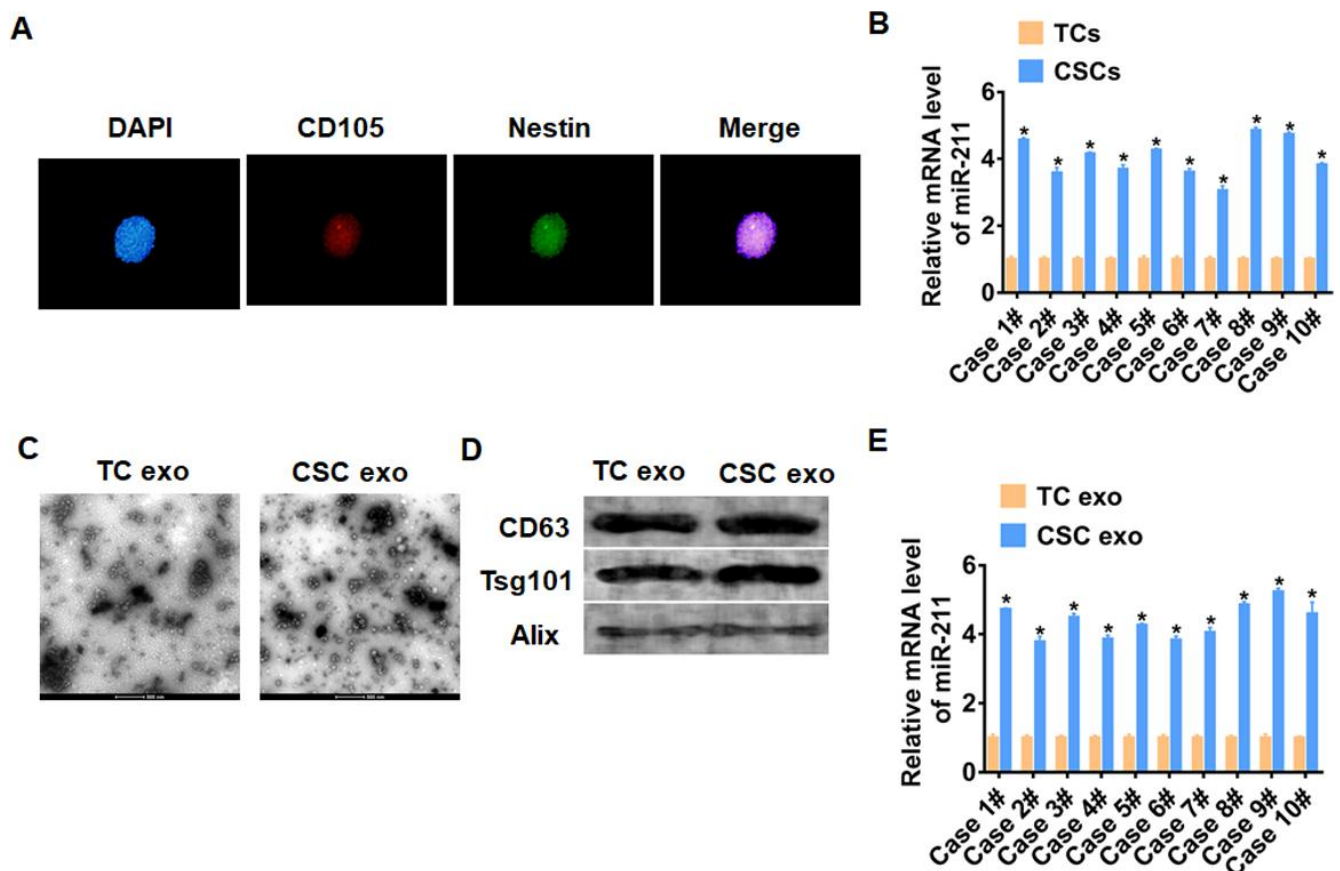


**Figure 1. CSCs secreted exosomal miR-211 in NSCLC.** (A) Immunofluorescence staining for CD105 and Nestin expression of CSCs 3D sphere. DAPI indicates nucleus. Scale bar = 20  $\mu$ M. (B) qRT-PCR analyzed the expression of miR-211 in TCs and CSCs. n=6, \*p<0.05. (C) TEM of exosomes isolated from TC and CSC. Scale bar = 500 nM. (D) Western blot for CD63, Tsg101 and Alix in exosomes. (E) The expression of miR-211 in exosomes was tested by qRT-PCR. n=6, \*p<0.05.

si- BCL-W and incubated with exosomes from CSCs transfected with miR-211 or AMO-211, respectively. Western blot assay showed that overexpression of BCL-W increased p62 expression and decreased LC3-II expression, which reversed pro-autophagic role of miR-211 in A549 and H1299 cells (Figure 5A). Similarly, silencing of BCL-W inhibited p62 level and

promoted LC3-II level, which remitted the function of AMO-211 (Figure 5B). Followed functional experiments showed that overexpression of BCL-W reduced cell viability, migration and invasion in A549 and H1299 cells (Figure 5C, 5E, 5G), while silencing of BCL-W showed the opposite function (Figure 5D, 5F, 5H).

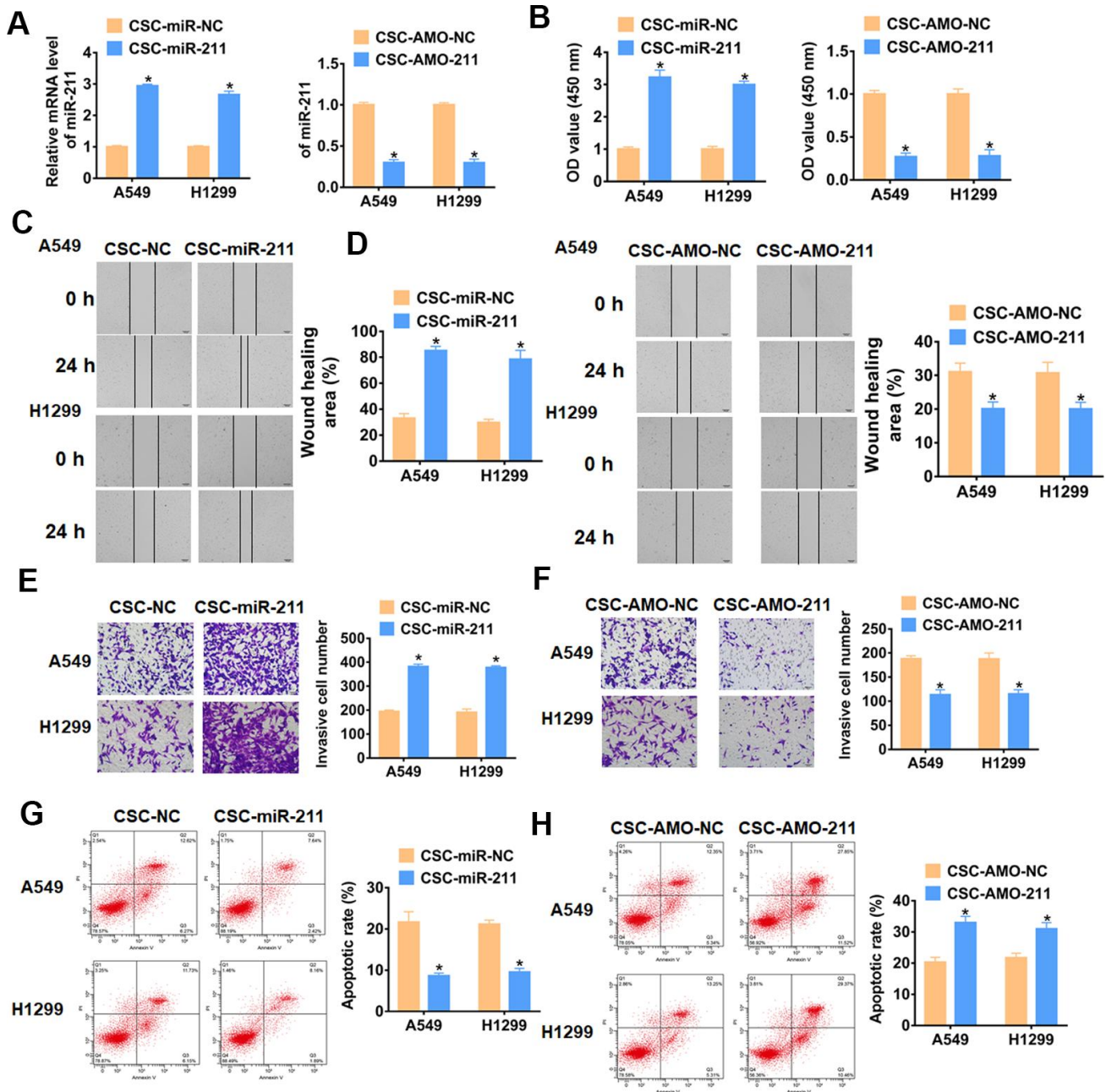


**Figure 2. Exo-miR-211 derived from CSCs accelerate cancer progression of NSCLC cells.** A549 and H1299 cells were incubated with exosomes isolated from CSCs transfected with miR-211 or AMO-211 or its NC. (A) qRT-PCR analyzed the expression of miR-211 A549 and H1299 cells. n=6, \*p<0.05 vs CSC-miR-NC or CSC-AMO-NC. (B) CCK8 was used to test viability of A549 and H1299 cells. n=10, \*p<0.05 vs CSC-miR-NC or CSC-AMO-NC. (C, D) Wound healing assay to detect migration ability. n=4, \*p<0.05 vs CSC-miR-NC or CSC-AMO-NC. (E, F) Transwell assay to detect invasion ability. n=4, \*p<0.05 vs CSC-miR-NC or CSC-AMO-NC. (G, H) The number of apoptotic cells was calculated by flow cytometry. n=6, \*p<0.05 vs CSC-miR-NC or CSC-AMO-NC.

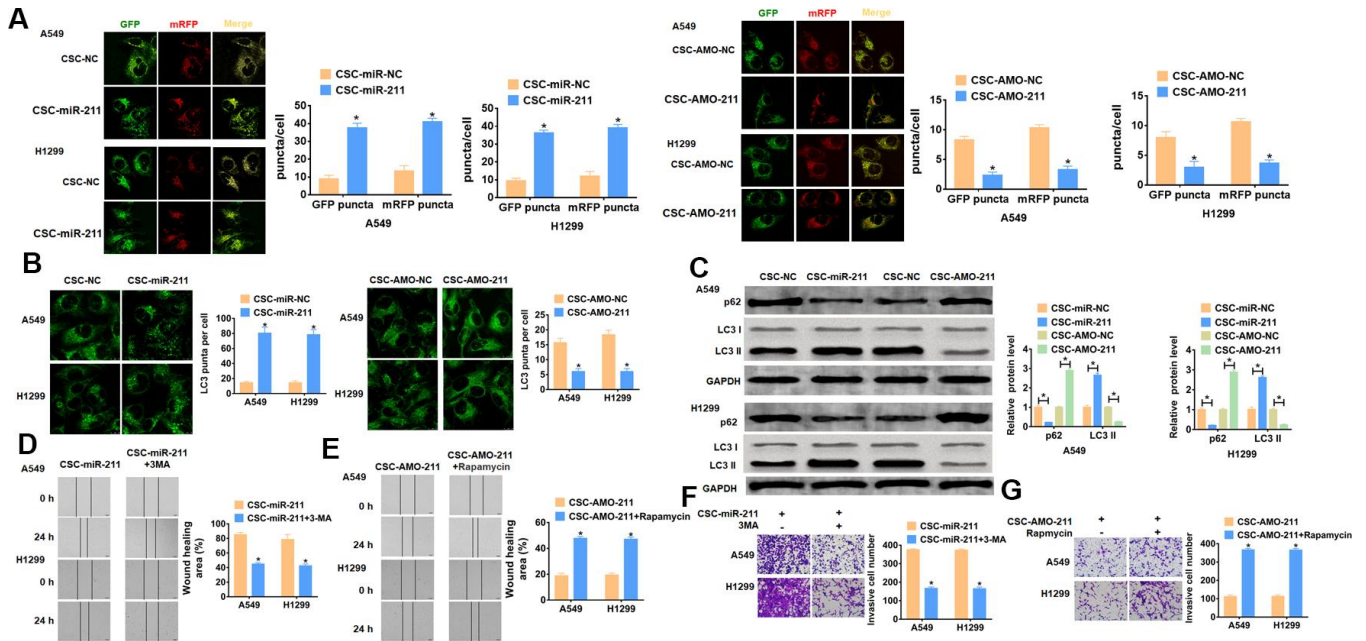


**Figure 3. Exo-miR-211 promotes cancer progression by activating autophagy of NSCLC cells.** (A) confocal microscope analysis for A549 and H1299 cells transfected with GFP-mRFP LC3.  $n=10$ ,  $*p<0.05$  vs CSC-miR-NC or CSC-AMO-NC. Scale bar = 100  $\mu$ m. (B) Western blot for autophagic associated proteins p62 and LC3I/II in A549 and H1299 cells.  $n=6$ ,  $*p<0.05$  vs CSC-miR-NC or CSC-AMO-NC. A549 and H1299 cells were treated with 3-MA (5  $\mu$ M) or rapamycin (50 nM).  $*p<0.05$  vs CSC-miR-NC or CSC-AMO-NC. (C–E) Wound healing assay to detect migration ability.  $n=4$ ,  $*p<0.05$  vs CSC-miR-211 or CSC-AMO-211. (F, G) Transwell assay to detect invasion ability.  $n=4$ ,  $*p<0.05$  vs CSC-miR-211 or CSC-AMO-211.

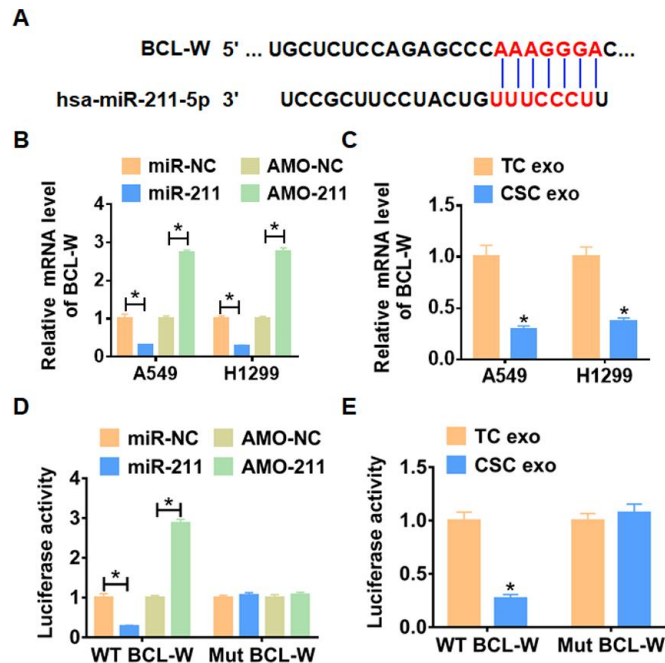


**Figure 4. miR-211 directly targeted on BCL-W in NSCLC cells.** (A) TargetScan predicted data between miR-211 and BCL-W. (B) qRT-PCR analyzed the expression of BCL-W in A549 and H1299 cells transfected with miR-211 or AMO-211.  $n=6$ ,  $*p<0.05$ . (C) qRT-PCR analyzed BCL-W expression of A549 and H1299 cells incubated with TC or CSC exosomes.  $n=6$ ,  $*p<0.05$  vs TC exo. (D) Luciferase assay for WT and mutant BCL-W activity in HEK293 cells transfected with miR-211 or AMO-211.  $n=6$ ,  $*p<0.05$ . (E) Luciferase assay for WT and mutant BCL-W activity in HEK293 cells incubated with TC or CSC exosomes.  $n=6$ ,  $*p<0.05$  vs TC exo.

## CSC-derived exo-miR-211 promoted NSCLC progression *in vivo*

The role of CSC-derived exo-miR-211 in NSCLC progression were further evaluated *in vivo*. CSCs stably transfected with miR-211 or AMO-211 or NC were constructed, and the nude mice were injected A549 or H1299 cells incubated with a mixture of CSCs (n = 6 for each group). Tumors grew faster and bigger in the mice with CSCs-miR-211, while CSCs-AMO-211 inhibited the growth rate and volume of tumors (Figure 6A). The tumors were isolated at 30 days after injection, CSCs-miR-211 significantly increased tumors weight, and CSCs-AMO-211 decreased tumors weight (Figure 6B). In addition, miR-211 decreased the mRNA expression of BCL-W in tumor tissues, while AMO-211 showed the opposite effect (Figure 6C). Moreover, miR-211 inhibited p62 expression and increased LC3-II expression, while AMO-211 showed the opposite effect in A549 and H1299 cells (Figure 6C).

## DISCUSSION

NSCLC is a highly lethal malignant tumor in the world today [1]. Despite the increasing knowledge of biomedical knowledge, the clinical prognosis of patients with advanced NSCLC is still unsatisfactory, and its five-year survival rate is less than 15% [22]. In fact, the survival rate of cancer patients has declined dramatically from early to late stages. Thus, it is urgent to look for targeted molecules for the prevention, diagnosis and treatment of NSCLC.

Exosomes originate from multivesicular bodies of nano-scale lipid membrane vesicles. At present, non-coding RNAs (ncRNAs) are commonly found in the exosomes of NSCLC patients. Especially, exosomal microRNAs are reported to be involved in the formation and evolution of tumors and play a significant role in the diagnosis and prognosis of NSCLC patients [23]. At

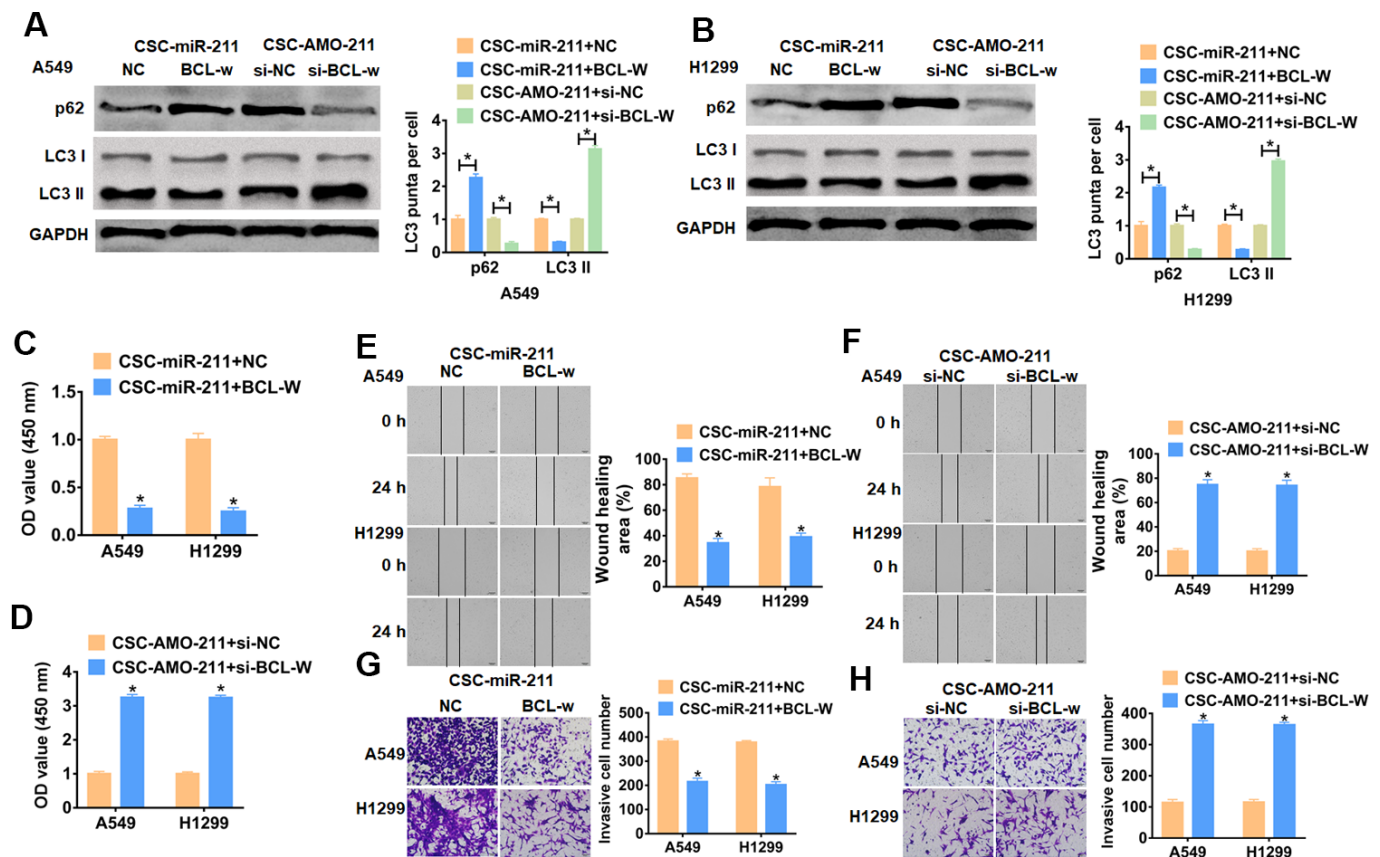


**Figure 5. miR-211 promotes cancer development by inhibiting BCL-W.** A549 and H1299 cells were transfected with BCL-W or si-BCL-W and incubated with exosomes from CSCs transfected with miR-211 or AMO-211, respectively. (A, B) Western blot for autophagic associated proteins p62 and LC3I/II in A549 and H1299 cells. n=6, \*p<0.05. (C, D) CCK8 was used to test viability of A549 and H1299 cells. n=10, \*p<0.05 vs CSC-miR-211+NC or CSC-AMO-211+si-NC. (E, F) Wound healing assay to detect migration ability. n=4, \*p<0.05 vs CSC-miR-211+NC or CSC-AMO-211+si-NC. (G, H) Transwell assay to detect invasion ability. n=4, \*p<0.05 vs CSC-miR-211+NC or CSC-AMO-211+si-NC.

present, with the help of NGS and gene chips, it has been found that tumor-derived exosomal miRNAs have great value in the diagnosis of NSCLC. Rabinowits et al. [24] used exosomes as genetic material for the first time, and analyzed the differences between exosomal miRNAs in normal human serum and miRNAs in NSCLC patients' serum. Although no significant differences were found in this study, it laid the foundation for future research to identify tumor molecular levels. Cazzoli et al. [25] found that the levels of miR-378, miR-502-5p, miR-629, miR-200b-5p and miR-100 were significantly higher in the peripheral blood of patients with lung adenocarcinoma than in patients with pulmonary granulomas and healthy patients.

CSCs have the biological characteristics of self-renewal, multi-directional differentiation, and infinite proliferation, and at the same time, they show resistance to chemotherapeutics, strong tumorigenicity, and strong invasion and metastasis [26]. Therefore, the proposal of

the concept of tumor stem cells and the in-depth study of its related molecular mechanisms provided a more reasonable explanation for the occurrence, recurrence, invasion and metastasis of tumors, and brought new ideas for tumor treatment. In addition, CSCs are considered as an important source of exosomes [27]. It has been reported that CSC-exosomes maintains tumor heterogeneity and promotes tumor progression [28]. Likewise, we found that CSCs could secreted exosomes that contained miR-211. Furthermore, we identified the function of CSC derived exo-miR-211. Results showed CSC derived exo-miR-211 promoted viability, migration and invasion, and inhibited apoptosis in NSCLC cells.

Autophagy is the process of transporting macromolecules, damaged organelles and metabolites to the lysosome to degrade and generate energy materials for cell survival. Autophagy is conducive to the survival of lung cancer cells, promotes the occurrence and

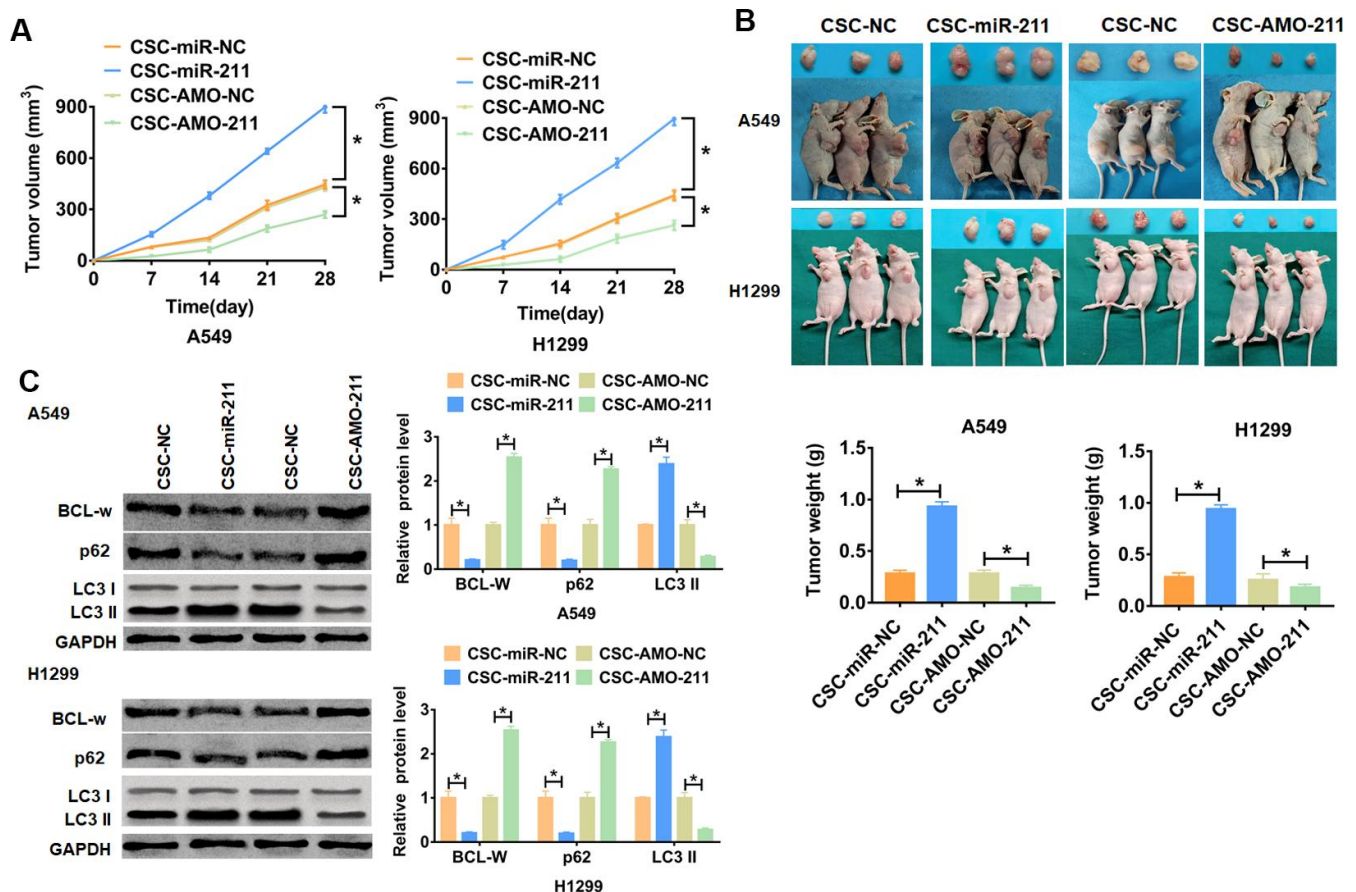


**Figure 6. Exo-miR-211 derived from CSC promoted tumorigenesis and autophagy of NSCLC cells *in vivo*.** CSCs stably transfected with miR-211 or AMO-211 or NC were constructed, and the nude mice were injected A549 or H1299 cells incubated with a mixture of CSCs (n = 6 for each group). (A) Growth of tumor xenografts in nude mice. n=6, \*p<0.05. (B) Representative tumors excised from xenografts in nude mice and tumor weight. n=6, \*p<0.05. (C) The protein expression of BCL-W and autophagy related protein p62 and LC3I/II were analyzed by western bolt in isolated tumors. n=6, \*p<0.05.

development of NSCLC [29]. In present study, LC3 and p62 expression were detected to assess autophagy level. Interestingly, CSC derived exo-miR-211 induced autophagy in NSCLC cells. What's more, autophagy inhibitor 3-MA removed the promoted effect of CSCs transfected with miR-211 on migration and invasion in A549 and H1299 cells. On the contrary, autophagy inducer Rapamycin recovered the inhibited effect of CSCs transfected with AMO-211 on migration and invasion in A549 and H1299 cells. These data indicated that exosomal miR-211 derived from CSCs promoted NSCLC development via activating autophagy.

BCL-W is a member of the Bcl-2 family, which plays a key role in the occurrence and development of many malignant tumors [30]. The cross talk between Bcl-2 family and Beclin 1 promotes autophagy [31]. As well, inhibition of BCL-W suppressed autophagy [32]. In present study, we surprisingly found that BCL-W was a direct target of miR-211. Furthermore, over expression of BCL-W reversed the effect of exo-miR-211 on promoting NSCLC progression and inducing autophagy. Meanwhile, *in vivo* tumor formation experiments proved that CSCs derived exo-miR-211 could significantly promoted the progression of NSCLC, which was conducive to clinical targeted therapy.

## CONCLUSIONS

Our study suggested CSCs derived exo-miR-211 promoted NSCLC progression by activating autophagy via targeting BCL-W.

## MATERIALS AND METHODS

### Clinical samples

Fresh cancer tissue samples and para-carcinoma tissue samples were taken from 15 NSCLC patients undergoing surgical procedures at Qingdao Haici medical group. All of the patients or their guardians provided written consent, and the Ethics Committee of Hiser Medical Center of Qingdao.

### CSCs and exosome isolation and identification

CSCs and TCs were isolated from cancer and para-carcinoma tissues of NSCLC patients as previously described [33]. Briefly, each NSCLC tissue specimen was minced into 1 mm<sup>3</sup> cube chunks and enzymatically dissociated to single cells. Cells were isolated and identified with CD105 and Nestin. Exosomes in culture medium, and several centrifugations were performed to purify exosomes. Transmission electron microscopy (TEM) was used to identify exosomes structures. CSCs-

derived exosomes were analyzed using exosome marker protein CD63, Tsg101 and ALIX via Western blot.

### Cell culture and treatment

The A549 and H1299 lines were purchased from the Science Cell Laboratory. Cells were cultured in RPMI 1640 supplemented with 10 % fetal bovine serum and 100 µL/mL penicillin and streptomycin. 2 µg plasmid or 500 nM si-RNA/miR-211/antisense morpholino oligonucleotide of miR-211 (AMO-211) or its NC was transfected into cells with Lipo 2000, respectively. Cells were treated with 3-MA (5 µM) or rapamycin (50 nM) for 1 h prior to co-culture assay. As for co-culture assay, we used transwell membranes in 12-well plates. CSCs or TCs were plated into the upper chamber, and A549 and H1299 was cultured in lower chamber.

### RNA isolation and qRT-PCR

RNA isolation, reverse transcription and quantitative expression were carried according to manufacturer's instructions after 36 h of transfection. All the kits were purchased from Vazyme, and gene expression was calculated using 2<sup>-ΔΔCt</sup> method. The relative expression level of miR-211 was calculated through normalization to U6 internal controls, and mRNAs were normalized with Actin.

### Protein isolation and western blot

Total protein was collected from cells with RIPA lysis Mix after 48 h of transfection. Western blotting assay was performed as previously described. Briefly, 60 µg protein extractions were loaded via SDS-PAGE and transferred onto nitrocellulose membranes (absin, China), then incubated with primary antibodies for 2 h at temperature, then plated at 4 °C overnight, the membranes were incubated in 5% non-fat milk blocking buffer for horizontal mode 3 h. After incubation with secondary antibodies, the membranes were scanned using an Odyssey, and data were analyzed with Odyssey software (LI-COR, USA). Primary antibodies list: CD63 (Abcam, ab217345), Tsg101 (Abcam, ab125011), Alix (Abcam, ab117600), LC3I/II (Sigma-Aldrich, L7543) and p62 (Sigma-Aldrich, 103M4785V), GAPDH (Proteintech, 60004-1-Ig).

### Immunofluorescence staining

Cells were plated in a 24-well cell culture plate. After transfection, cells were washed by PBS and fixed with 4% paraformaldehyde. Cells were permeabilized with 0.2% Triton-X-100 solution in PBS. Next, we blocked cell using goat serum. Then, the cells were incubated antibody at 4 °C overnight followed with second

antibodies incubation for 1h. After three washes with PBS, we incubated cells by DAPI.

### Luciferase assay

psiCHECK-2 luciferase reporter plasmid was inserted with the wildtype BCL-W 3'UTR or mutant 3'UTR sequences, then were transfected with reporter vectors into HEK293 cells. The cells were collected after 48 h post-transfection and lysed to detected the luciferase activity (Promega).

### CCK8 assay

Cells were seeded in 96-well cell plates, and added CCK-8 solution (Vazyme, China) at 48 h. 2 hours later, measure the OD value at 450 nm.

### Wound healing assay

$5 \times 10^5$  cells were planted in a 6-well plate, and when the cells grew to fuse, two vertical parallel lines were drawn with 10  $\mu$ L suction head against the ruler. The floating cells were washed with PBS and cultured in serum-free medium for 24 hours. Images were taken at 0 and 24 hours of cell culture, respectively.

### Transwell assay

Cells in logarithmic growth phase were adjusted to  $2 \times 10^5$  cells/well of medium (without serum) and plated into the upper chamber insert pre-coated with 1 $\mu$ g/ $\mu$ L Matrigel. Lower chamber was added with 500  $\mu$ L of medium (with 10% FBS), and then incubate the chamber at 37°C for 48 h. Then the invading cells were visualized by the crystal violet and inverted microscope.

### Cell apoptosis assay

Cell apoptosis was calculated by Annexin V apoptosis kit (Beyotime, China), and the operating procedure was according to the kit instructions. Briefly,  $5 \times 10^5$  cells/mL were centrifuged and resuspended in Binding Buffer containing Annexin V-FITC and PI. Cell apoptosis level was detected within 1 h in Binding Buffer.

### *In vivo* tumor growth assay

Nude mice were purchased from Guangdong provincial experimental animal center for medicine. CSCs stably transfected with miR-211 or AMO-211 or NC were constructed, and the nude mice were injected A549 or H1299 cells incubated with a mixture of CSCs (n = 6 for each group). Tumor size was measured every 7 days. After 28 days of injection, mice were

intraperitoneally injected with 3% pentobarbital sodium and were killed by excessive anesthesia with a dose of 90 mL/kg, and the tumors were removed for follow-up study. This study was reviewed and approved by animal experimental ethics committee of Hiser Medical Center of Qingdao.

### Statistical analysis

Significant differences were calculated using two-tailed t-test through Graphpad 7.0 and SPSS 22.0. For two group comparisons, Student t-test was used. For multiple group comparisons, one-way ANOVA was used with Bonferroni post-test for comparisons between selected two groups as well as Dunnett post-test for comparisons among all other treatment groups to the corresponding control. A value  $p < 0.05$  was considered statistically significant.

### CONFLICTS OF INTEREST

The authors declare no conflicts of interest.

### REFERENCES

1. Zhang R, Cai L, Wang G, Wen Y, Wang F, Zhou N, Zhang X, Huang Z, Yu X, Xi K, Yang L, Zhao D, Lin Y, Zhang L. Resection of early-stage second primary non-small cell lung cancer after small cell lung cancer: a population-based study. *Front Oncol.* 2020; 9:1552. <https://doi.org/10.3389/fonc.2019.01552> PMID:[32117785](https://pubmed.ncbi.nlm.nih.gov/32117785/)
2. Murray SR, Murchie P, Campbell N, Walter FM, Mazza D, Habgood E, Kutzer Y, Martin A, Goodall S, Barnes DJ, Emery JD. Protocol for the CHEST Australia trial: a phase II randomised controlled trial of an intervention to reduce time-to-consult with symptoms of lung cancer. *BMJ Open.* 2015; 5:e008046. <https://doi.org/10.1136/bmjopen-2015-008046> PMID:[25986641](https://pubmed.ncbi.nlm.nih.gov/25986641/)
3. Saad MI, Rose-John S, Jenkins BJ. ADAM17: an emerging therapeutic target for lung cancer. *Cancers (Basel).* 2019; 11:1218. <https://doi.org/10.3390/cancers11091218> PMID:[31438559](https://pubmed.ncbi.nlm.nih.gov/31438559/)
4. Yao RQ, Ren C, Xia ZF, Yao YM. Organelle-specific autophagy in inflammatory diseases: a potential therapeutic target underlying the quality control of multiple organelles. *Autophagy.* 2020; 1–17. <https://doi.org/10.1080/15548627.2020.1725377> PMID:[32048886](https://pubmed.ncbi.nlm.nih.gov/32048886/)
5. Pagotto A, Pilotto G, Mazzoldi EL, Nicoletto MO, Frezzini S, Pastò A, Amadori A. Autophagy inhibition reduces chemoresistance and tumorigenic potential of

- human ovarian cancer stem cells. *Cell Death Dis.* 2017; 8:e2943.  
<https://doi.org/10.1038/cddis.2017.327>  
 PMID:[28726781](https://pubmed.ncbi.nlm.nih.gov/28726781/)
6. Guo JY, Teng X, Laddha SV, Ma S, Van Nostrand SC, Yang Y, Khor S, Chan CS, Rabinowitz JD, White E. Autophagy provides metabolic substrates to maintain energy charge and nucleotide pools in ras-driven lung cancer cells. *Genes Dev.* 2016; 30:1704–17.  
<https://doi.org/10.1101/gad.283416.116>  
 PMID:[27516533](https://pubmed.ncbi.nlm.nih.gov/27516533/)
  7. Karsli-Uzunbas G, Guo JY, Price S, Teng X, Laddha SV, Khor S, Kalaany NY, Jacks T, Chan CS, Rabinowitz JD, White E. Autophagy is required for glucose homeostasis and lung tumor maintenance. *Cancer Discov.* 2014; 4:914–27.  
<https://doi.org/10.1158/2159-8290.CD-14-0363>  
 PMID:[24875857](https://pubmed.ncbi.nlm.nih.gov/24875857/)
  8. White E. Deconvoluting the context-dependent role for autophagy in cancer. *Nat Rev Cancer.* 2012; 12:401–10.  
<https://doi.org/10.1038/nrc3262>  
 PMID:[22534666](https://pubmed.ncbi.nlm.nih.gov/22534666/)
  9. Xie M, Xiong W, She Z, Wen Z, Abdirahman AS, Wan W, Wen C. Immunoregulatory effects of stem cell-derived extracellular vesicles on immune cells. *Front Immunol.* 2020; 11:13.  
<https://doi.org/10.3389/fimmu.2020.00013>  
 PMID:[32117221](https://pubmed.ncbi.nlm.nih.gov/32117221/)
  10. Liu X, Miao J, Wang C, Zhou S, Chen S, Ren Q, Hong X, Wang Y, Hou FF, Zhou L, Liu Y. Tubule-derived exosomes play a central role in fibroblast activation and kidney fibrosis. *Kidney Int.* 2020; 97:1181–95.  
<https://doi.org/10.1016/j.kint.2019.11.026>  
 PMID:[32139089](https://pubmed.ncbi.nlm.nih.gov/32139089/)
  11. Khan N, Mironov G, Berezovski MV. Direct detection of endogenous MicroRNAs and their post-transcriptional modifications in cancer serum by capillary electrophoresis-mass spectrometry. *Anal Bioanal Chem.* 2016; 408:2891–99.  
<https://doi.org/10.1007/s00216-015-9277-y>  
 PMID:[26769131](https://pubmed.ncbi.nlm.nih.gov/26769131/)
  12. Thakur BK, Zhang H, Becker A, Matei I, Huang Y, Costa-Silva B, Zheng Y, Hoshino A, Brazier H, Xiang J, Williams C, Rodriguez-Barrueco R, Silva JM, et al. Double-stranded DNA in exosomes: a novel biomarker in cancer detection. *Cell Res.* 2014; 24:766–69.  
<https://doi.org/10.1038/cr.2014.44>  
 PMID:[24710597](https://pubmed.ncbi.nlm.nih.gov/24710597/)
  13. Yáñez-Mó M, Siljander PR, Andreu Z, Zavec AB, Borràs FE, Buzas EI, Buzas K, Casal E, Cappello F, Carvalho J, Colás E, Cordeiro-da Silva A, Fais S, et al. Biological properties of extracellular vesicles and their physiological functions. *J Extracell Vesicles.* 2015; 4:27066.  
<https://doi.org/10.3402/jev.v4.27066> PMID:[25979354](https://pubmed.ncbi.nlm.nih.gov/25979354/)
  14. Koren E, Fuchs Y. The bad seed: cancer stem cells in tumor development and resistance. *Drug Resist Updat.* 2016; 28:1–12.  
<https://doi.org/10.1016/j.drug.2016.06.006>  
 PMID:[27620951](https://pubmed.ncbi.nlm.nih.gov/27620951/)
  15. Lytle NK, Barber AG, Reya T. Stem cell fate in cancer growth, progression and therapy resistance. *Nat Rev Cancer.* 2018; 18:669–80.  
<https://doi.org/10.1038/s41568-018-0056-x>  
 PMID:[30228301](https://pubmed.ncbi.nlm.nih.gov/30228301/)
  16. Zhang X, Shi H, Yuan X, Jiang P, Qian H, Xu W. Tumor-derived exosomes induce N2 polarization of neutrophils to promote gastric cancer cell migration. *Mol Cancer.* 2018; 17:146.  
<https://doi.org/10.1186/s12943-018-0898-6>  
 PMID:[30292233](https://pubmed.ncbi.nlm.nih.gov/30292233/)
  17. Song M, Wang Y, Shang ZF, Liu XD, Xie DF, Wang Q, Guan H, Zhou PK. Bystander autophagy mediated by radiation-induced exosomal miR-7-5p in non-targeted human bronchial epithelial cells. *Sci Rep.* 2016; 6:30165.  
<https://doi.org/10.1038/srep30165>  
 PMID:[27417393](https://pubmed.ncbi.nlm.nih.gov/27417393/)
  18. Xiao H. MiR-7-5p suppresses tumor metastasis of non-small cell lung cancer by targeting NOVA2. *Cell Mol Biol Lett.* 2019; 24:60.  
<https://doi.org/10.1186/s11658-019-0188-3>  
 PMID:[31832068](https://pubmed.ncbi.nlm.nih.gov/31832068/)
  19. Xu F, Zhong JY, Lin X, Shan SK, Guo B, Zheng MH, Wang Y, Li F, Cui RR, Wu F, Zhou E, Liao XB, Liu YS, Yuan LQ. Melatonin alleviates vascular calcification and ageing through exosomal miR-204/miR-211 cluster in a paracrine manner. *J Pineal Res.* 2020; 68:e12631.  
<https://doi.org/10.1111/jpi.12631>  
 PMID:[31943334](https://pubmed.ncbi.nlm.nih.gov/31943334/)
  20. Bu Y, Yoshida A, Chitnis N, Altman BJ, Tameire F, Oran A, Gennaro V, Armeson KE, McMahon SB, Wertheim GB, Dang CV, Ruggero D, Koumenis C, et al. A PERK-miR-211 axis suppresses circadian regulators and protein synthesis to promote cancer cell survival. *Nat Cell Biol.* 2018; 20:104–15.  
<https://doi.org/10.1038/s41556-017-0006-y>  
 PMID:[29230015](https://pubmed.ncbi.nlm.nih.gov/29230015/)
  21. Gan X, Zhu H, Jiang X, Obiegbusi SC, Yong M, Long X, Hu J. CircMUC16 promotes autophagy of epithelial ovarian cancer via interaction with ATG13 and miR-199a. *Mol Cancer.* 2020; 19:45.  
<https://doi.org/10.1186/s12943-020-01163-z>  
 PMID:[32111227](https://pubmed.ncbi.nlm.nih.gov/32111227/)

22. Garon EB, Hellmann MD, Rizvi NA, Carcereny E, Leigh NB, Ahn MJ, Eder JP, Balmanoukian AS, Aggarwal C, Horn L, Patnaik A, Gubens M, Ramalingam SS, et al. Five-year overall survival for patients with advanced Non-Small-cell lung cancer treated with pembrolizumab: results from the phase I KEYNOTE-001 study. *J Clin Oncol*. 2019; 37:2518–27. <https://doi.org/10.1200/JCO.19.00934> PMID:[31154919](https://pubmed.ncbi.nlm.nih.gov/31154919/)
23. Wei F, Ma C, Zhou T, Dong X, Luo Q, Geng L, Ding L, Zhang Y, Zhang L, Li N, Li Y, Liu Y. Exosomes derived from gemcitabine-resistant cells transfer Malignant phenotypic traits via delivery of miRNA-222-3p. *Mol Cancer*. 2017; 16:132. <https://doi.org/10.1186/s12943-017-0694-8> PMID:[28743280](https://pubmed.ncbi.nlm.nih.gov/28743280/)
24. Rabinowits G, Gerçel-Taylor C, Day JM, Taylor DD, Kloecker GH. Exosomal microRNA: a diagnostic marker for lung cancer. *Clin Lung Cancer*. 2009; 10:42–46. <https://doi.org/10.3816/CLC.2009.n.006> PMID:[19289371](https://pubmed.ncbi.nlm.nih.gov/19289371/)
25. Cazzoli R, Buttitta F, Di Nicola M, Malatesta S, Marchetti A, Rom WN, Pass HI. microRNAs derived from circulating exosomes as noninvasive biomarkers for screening and diagnosing lung cancer. *J Thorac Oncol*. 2013; 8:1156–62. <https://doi.org/10.1097/JTO.0b013e318299ac32> PMID:[23945385](https://pubmed.ncbi.nlm.nih.gov/23945385/)
26. Sharifzad F, Ghavami S, Verdi J, Mardpour S, Mollapour Sisakht M, Azizi Z, Taghikhani A, Łos MJ, Fakharian E, Ebrahimi M, Hamidieh AA. Glioblastoma cancer stem cell biology: potential theranostic targets. *Drug Resist Updat*. 2019; 42:35–45. <https://doi.org/10.1016/j.drug.2018.03.003> PMID:[30877905](https://pubmed.ncbi.nlm.nih.gov/30877905/)
27. Yang Z, Zhao N, Cui J, Wu H, Xiong J, Peng T. Exosomes derived from cancer stem cells of gemcitabine-resistant pancreatic cancer cells enhance drug resistance by delivering miR-210. *Cell Oncol (Dordr)*. 2020; 43:123–36. <https://doi.org/10.1007/s13402-019-00476-6> PMID:[31713003](https://pubmed.ncbi.nlm.nih.gov/31713003/)
28. Sharma A. Role of stem cell derived exosomes in tumor biology. *Int J Cancer*. 2018; 142:1086–92. <https://doi.org/10.1002/ijc.31089> PMID:[28983919](https://pubmed.ncbi.nlm.nih.gov/28983919/)
29. Cao Q, You X, Xu L, Wang L, Chen Y. PAQR3 suppresses the growth of non-small cell lung cancer cells via modulation of EGFR-mediated autophagy. *Autophagy*. 2020; 16:1236–47. <https://doi.org/10.1080/15548627.2019.1659654> PMID:[31448672](https://pubmed.ncbi.nlm.nih.gov/31448672/)
30. Liu SH, Wang PP, Chen CT, Li D, Liu QY, Lv L, Liu X, Wang LN, Li BX, Weng CY, Fang XS, Cao XF, Mao HB, et al. MicroRNA-148b enhances the radiosensitivity of b-cell lymphoma cells by targeting bcl-w to promote apoptosis. *Int J Biol Sci*. 2020; 16:935–46. <https://doi.org/10.7150/ijbs.40756> PMID:[32140063](https://pubmed.ncbi.nlm.nih.gov/32140063/)
31. Erlich S, Mizrachy L, Segev O, Lindenboim L, Zmira O, Adi-Harel S, Hirsch JA, Stein R, Pinkas-Kramarski R. Differential interactions between beclin 1 and bcl-2 family members. *Autophagy*. 2007; 3:561–68. <https://doi.org/10.4161/auto.4713> PMID:[17643073](https://pubmed.ncbi.nlm.nih.gov/17643073/)
32. Crawford AC, Riggins RB, Shajahan AN, Zwart A, Clarke R. Co-inhibition of BCL-W and BCL2 restores antiestrogen sensitivity through BECN1 and promotes an autophagy-associated necrosis. *PLoS One*. 2010; 5:e8604. <https://doi.org/10.1371/journal.pone.0008604> PMID:[20062536](https://pubmed.ncbi.nlm.nih.gov/20062536/)
33. Bussolati B, Bruno S, Grange C, Ferrando U, Camussi G. Identification of a tumor-initiating stem cell population in human renal carcinomas. *FASEB J*. 2008; 22:3696–705. <https://doi.org/10.1096/fj.08-102590> PMID:[18614581](https://pubmed.ncbi.nlm.nih.gov/18614581/)